

A Gigabit-Per-Second Ka-band Demonstration Using A Reconfigurable FPGA Modulator

Dennis Lee, Andrew Gray, Edward Kang, Haiping Tsou, Norman Lay
Jet Propulsion Laboratory
4800 Oak Grove Drive
Pasadena, CA 91109
(818) 354-4321

Wai Fong, Dave Fisher, Scott Hoy
Goddard Space Flight Center
Mailstop 567.0
Greenbelt, MD 20771
(301) 286-8165

Abstract—Gigabit-per-second communications have been a desired target for future NASA Earth science missions, and for potential manned lunar missions. Frequency bandwidth at S-band and X-band is typically insufficient to support missions at these high data rates. In this paper, we present the results of a 1 Gbps 32-QAM end-to-end experiment at Ka-band using a reconfigurable Field Programmable Gate Array (FPGA) baseband modulator board. Bit error rate measurements of the received signal using a software receiver demonstrate the feasibility of using ultra-high data rates at Ka-band, although results indicate that error correcting coding and/or modulator predistortion must be implemented in addition. Also, results of the demonstration validate the low-cost, CMOS-based reconfigurable modulator approach taken to development of a high rate modulator, as opposed to more expensive ASIC or pure analog approaches.^{1,2}

TABLE OF CONTENTS

1. INTRODUCTION.....	1
2. RECONFIGURABLE FPGA MODULATOR.....	2
3. KA-BAND CHANNEL	2
4. SOFTWARE RECEIVER.....	4
5. RESULTS AND DISCUSSION.....	5
6. CONCLUSION	7
REFERENCES	8
BIOGRAPHY	9

1. INTRODUCTION

Data rate requirements for current and future planned Earth science missions are rapidly escalating, with gigabit per second (Gbps) communications becoming a realistic target in the not-so-distant future. Furthermore, with the recent emphasis on manned lunar missions, high data rate communications from the Moon is very likely. However,

these high data rates place a strain on both the available frequency bandwidth and modulator/receiver hardware technology.

To accommodate the expansion in downlink telemetry rates, the International Telecommunications Union (ITU) has allocated the 25.5-27.0 GHz band (commonly referred to as the 26 GHz band) for Earth Exploration Satellite (EES) space-to-Earth links on a primary basis worldwide. Since only 375 MHz bandwidth is available in the X-band EES allocation, very high rate NASA missions will be forced to migrate to the 26 GHz Ka-band frequency band [1].

However, at gigabit-per-second data rates, even the 26 GHz band will only be able to support a few missions. This is particularly true for lunar missions where there may be several transmitters located in close proximity to each other, all competing for the same spectrum. Thus there is still a need for bandwidth efficient modulations. Higher order modulations such as 8-PSK, 16-QAM, and 32-QAM offer better bandwidth efficiency in terms of bits/sec/Hz, and more sophisticated pulse shaping methods can be used to reduce adjacent channel interference. However, hardware implementation of highly bandwidth efficient modulations at Gbps data rates entails design, specification, and evaluation challenges much greater than those based on traditional QPSK-type systems currently in operation. This area represents an opportunity for technology development for NASA.

In this paper, we present the results of a gigabit per second communications demonstration at 26 GHz using 32-Quadrature Amplitude Modulation (QAM) with Square Root Raised Cosine (SRRC) pulse shaping. The baseband 32-QAM signal is generated using a reconfigurable FPGA baseband modulator board architecture jointly developed by the Goddard Space Flight Center and the Jet Propulsion Laboratory [2]. The CMOS-based FPGA design carries advantages in both cost and flexibility.

¹ 0-7803-8870-4/05/\$20.00© 2005 IEEE

² IEEEAC paper #1403, Version 4, Updated December 10, 2004

This demonstration serves three purposes: (1) Establishes NASA's ability to create a 1 Gbps link at Ka-band using relatively low-cost high-rate bandwidth efficient modulator technology, (2) Validates the low-cost CMOS based bandwidth efficient reconfigurable modulator (with high bits/second/Hertz) developed by the authors in a laboratory setting at very high data rates thus raising the technology readiness level of the modulator with these modulations, and (3) Creates an extendable test platform that may be utilized in the future to gain knowledge about and validate a large array of modulations for use by NASA missions in a TRL-5 environment.

The remainder of this paper is divided into four sections. Section 2 describes the FPGA modulator board, Section 3 details the Ka-band channel used in the experimental testbed, and Section 4 describes the software receiver. Results from the demonstration are discussed in Section 5, and concluding remarks are presented in Section 6.

2. RECONFIGURABLE FPGA MODULATOR

The 32-QAM waveforms were implemented in a digital baseband modulator board jointly developed by GSFC and JPL [2]. It contains a single Xilinx XC2V6000 FPGA which performed the waveform generation, encoder logic, and digital filtering. Also contained on the board are two high speed Rockwell digital-to-analog converters (DAC's). A compact flash card was used to upload the VHDL configuration files into the Xilinx FPGA. A picture of the high rate digital modulator board is shown in Figure 1.

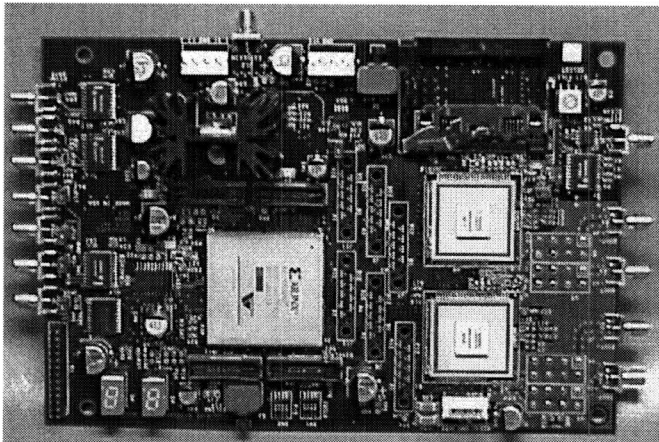


Figure 1 – High Rate Digital Baseband Modulator Board

The modulator board is currently capable of generating baseband waveforms for SRRC-shaped QPSK, GMSK, trellis-coded 8PSK, 16-QAM, and 32-QAM. It can also be expanded to include other modulation types such as Amplitude Phase Shift Keying (APSK). The 32-QAM waveforms are pulse shaped using a SRRC filter with roll-

off factor $\alpha=0.35$. Mathematically, the SRRC filter impulse response is given by:

$$h_{SRRC}(t) = \sqrt{\frac{\sin(\pi/T) \cos(\pi\alpha/T)}{\pi/T \cdot 1 - (4\alpha/T)^2}} \quad (1)$$

The SRRC response in the FPGA is truncated to eight symbols periods in duration.

For the targeted bit rate of 1 Gbps, the input clock to the DAC on the modulator board is 400 MHz. The DAC clock, which is supplied by an external frequency synthesizer, was divided down by two in the modulator board to produce a 200 MHz symbol clock for the 32-QAM waveform generation. Since there are 5 bits in each 32-QAM symbol, the transmitted bit rate was 1 Gbps. A parallel PN-sequence generator bank was added to the FPGA design to supply random input bits to the modulator and enable bit error rate measurements. A block diagram of the baseband modulator board can be seen in Figure 2.

Two 150 MHz filters were used to smooth the inphase (I) and quadrature phase (Q) output waveforms from the DAC. The baseband signals were then upconverted to a 1200 MHz IF frequency using an external I-Q modulator.

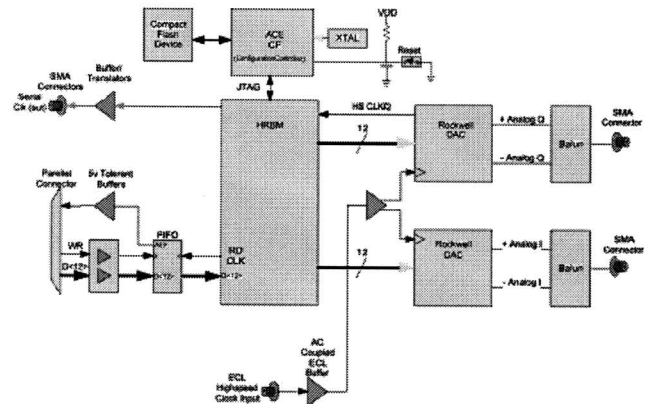


Figure 2 - Digital Baseband Modulator Functional Block Diagram

3. KA-BAND CHANNEL

The Ka-band channel in the experimental testbed consisted of a 25.5-27.5 GHz upconverter and down-converter, and a wideband 26.5-40.0 GHz Traveling Wave Tube Amplifier (TWTA). Figure 3 shows a block diagram of the end-to-end Ka-band demonstration testbed. The 1200 MHz IF signal from the FPGA modulator was upconverted to 26.7 GHz using a Miteq dual up/down-converter. The output of the upconverter was used to drive a Hughes 8001H 1W TWTA. The input backoff (IBO) of the TWTA was controlled using a variable Ka-band attenuator.

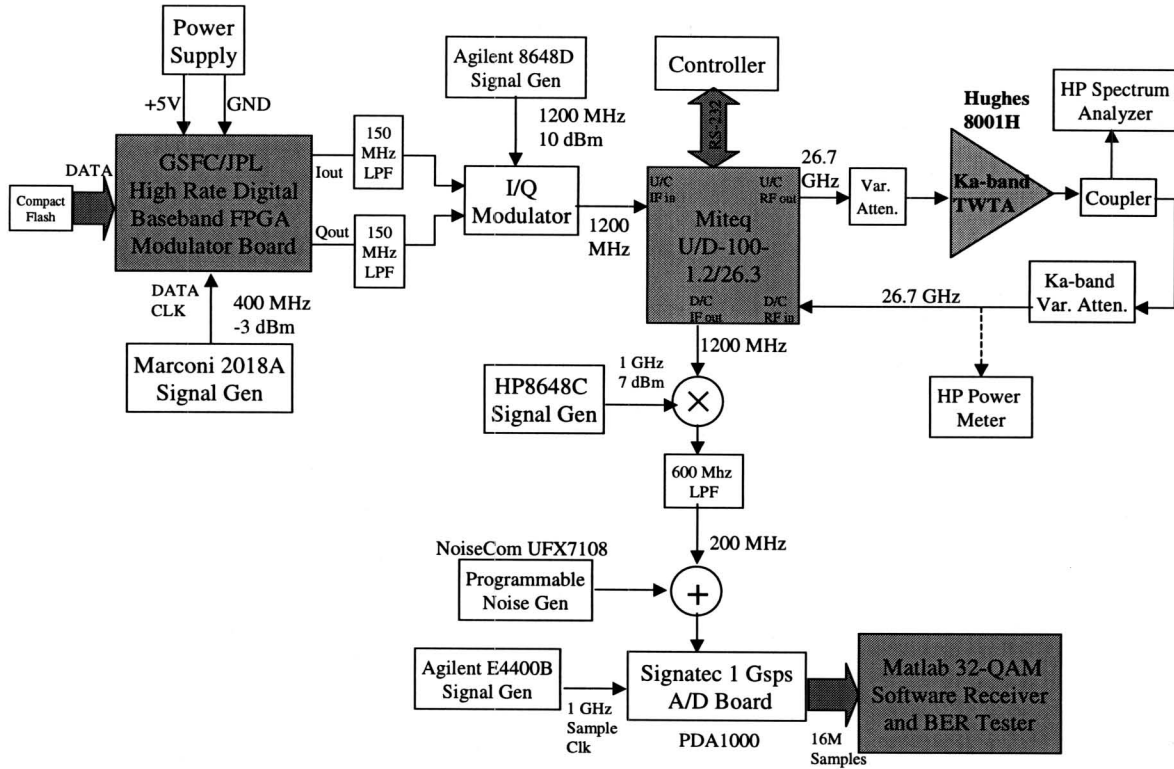


Figure 3 – Experimental Testbed Setup

The output of the TWTA was then downconverted back to 1200 MHz IF, and mixed down to 200 MHz where it was sampled using a 1 gigasample-per-second A/D board. The samples were stored in onboard RAM, and downloaded to a PC for demodulation and data post-processing. Bit error rate measurements were made using a software receiver. A NoiseCom programmable noise generator was used to adjust the signal-to-noise ratio.

Figure 4 shows the measured AM/AM characteristic of the Hughes 8001H TWTA. Operating the TWTA in the nonlinear region of the AM/AM curve provided more transmit power but introduced signal distortion and spectral growth of the 32-QAM signal. The degree of distortion is a function of the amplifier input backoff (IBO). In this paper, we define the input backoff of the operating point (defined here as the average power of the TWTA input drive level) with respect to the 1 dB compression point shown in Figure 4. The 1 dB compression point corresponds to an input drive level of about -14 dBm. As an example, -8 dB IBO would correspond to input drive power of -22 dBm which is clearly in the linear region of the amplifier. Likewise, the 3 dB compression point would correspond to an IBO of +5 dBm which is in the saturated region of the amplifier.

For the cross 32-QAM constellation [3] used in the demonstration (see Figure 7), the computed peak-to-average power ratio (PAPR) is 2.3 dB. The cross 32-QAM constellation was chosen instead of a rectangular

constellation because it has a lower PAPR. If operation in the strictly linear region of the TWTA is desired, it is necessary to further backoff the amplifier operating point by the PAPR amount to account for the peak power excursions. Thus using cross 32-QAM, -8 dB IBO is required for operation in the strictly linear region of this TWTA.

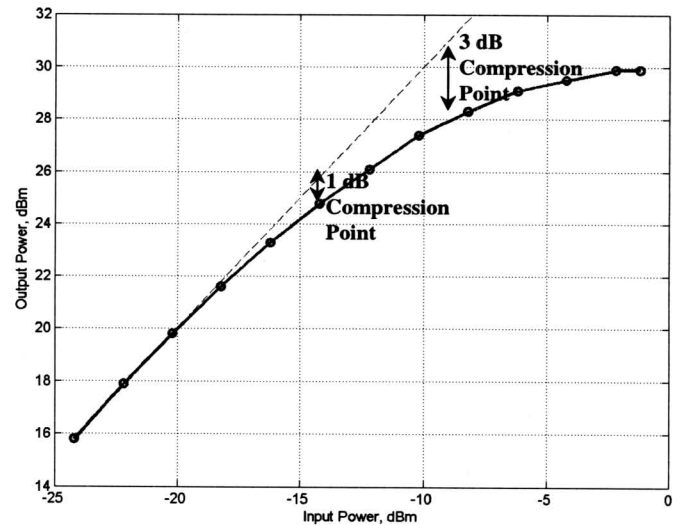
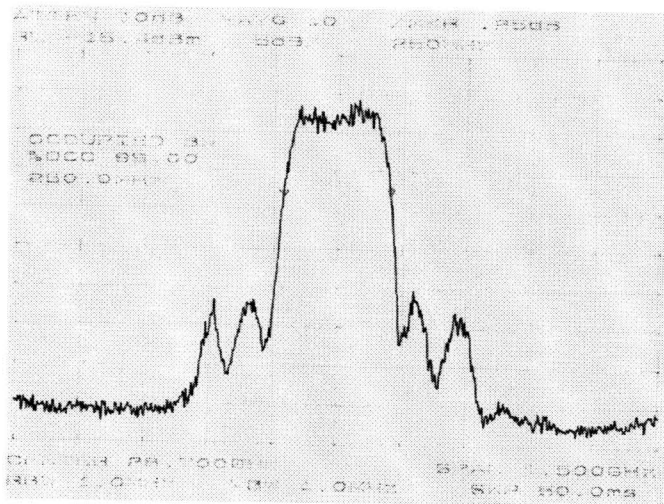
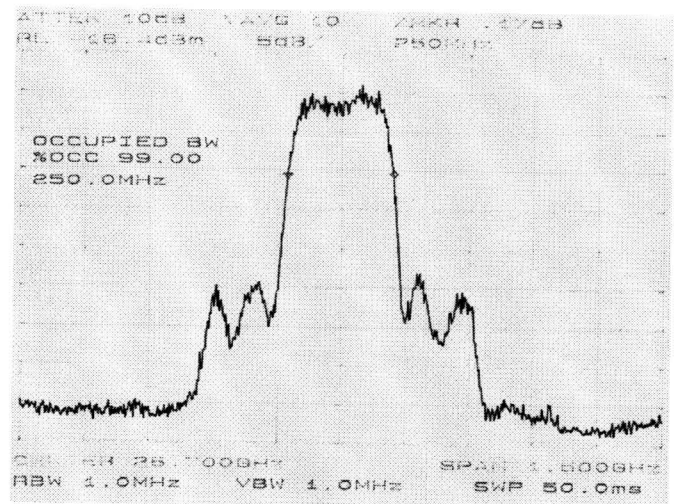


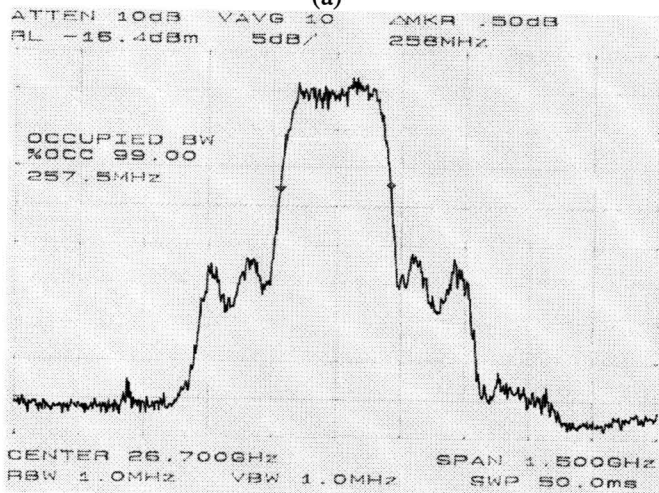
Figure 4 – Ka-band TWTA AM/AM Characteristic



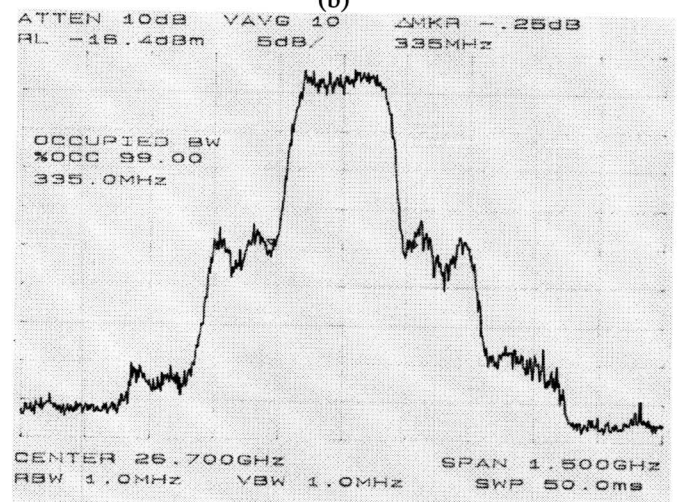
(a)



(b)



(c)



(d)

Figure 5 – SRRC 32-QAM Spectra at Output of TWTA: (a) with -2 dB IBO, (b) with 0 dB IBO, (c) with +2 dB IBO, and (d) with +5 dB IBO

Five different backoff cases were tested in this experiment. The first test case was -8 dB TWTA IBO (input power = -22 dBm) which represented strictly linear amplifier operation. The second case used an IBO of -2 dB (input power = -16 dBm), representing near linear operation of the TWTA with the peak power just exceeding the 1 dB compression point. The third case was 0 dB IBO (input power = -14 dBm) where the operating point was located directly at the 1 dB compression point. The last two cases were +2 dB IBO (input power = -12 dBm) and +5 dB IBO which represented saturated operation of the TWTA.

Figure 5 shows the measured spectra taken at the output of the TWTA for different IBO values. Note how the sidelobe levels grew as the operating point moved higher on the AM/AM curve. The null-to-null bandwidth of the SRRC 32-QAM main lobe at the output of the TWTA was approximately 310 MHz, which was slightly higher than the predicted theoretical bandwidth of 270 MHz due to modulator imperfections.

The occupied bandwidth of the signal (defined by the ITU Radio Regulations as the 99% power containment bandwidth) was approximately 250 MHz in the linear operating region of the TWTA, and expanded to almost 335 MHz at the 3 dB compression point. However, the occupied bandwidth did not significantly increase up to and including the 1 dB compression point. The measured 99% occupied bandwidth of the 32-QAM signal as a function of TWTA input backoff is summarized in Table 5.

4. SOFTWARE RECEIVER

The 32-QAM software receiver used in the experiment was programmed in Matlab, and utilized a fixed length training sequence for demodulation and equalization. Using a software receiver enabled analysis and processing of the received signal in non-realtime. The 32-QAM training sequence was 144 modulation symbols in length,

and was appended to the beginning of each transmitted packet by the FPGA modulator board. In this experiment, each packet contained 1246 symbols including the training sequence, but other packet length can be used with slight modifications to the VHDL code. Figure 6 shows the simple transmit packet structure used in the 1 Gbps 32-QAM demonstration.

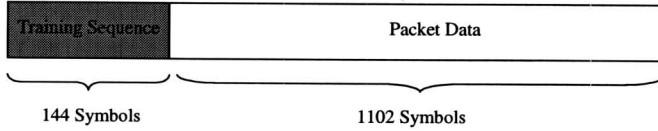


Figure 6 - Transmit Packet Structure

The software receiver performed SRRC matched filtering of the signal, and correlated the matched filter output with the training sequence to determine the beginning of the packet. Using the training sequence, the receiver also performed sample timing correction and estimation of the carrier phase rotation. The receiver also implemented Recursive Least Squares (RLS) decision-feedback equalization to compensate for channel distortions and intersymbol interference (ISI), and improve BER performance.

The cross 32-QAM constellation and symbol-to-bit mapping are shown in Figure 7. The symbol-to-bit mapping is a pseudo-Grey code. A bit error checking algorithm compared the detected bits to the transmitted PN sequence to determine the bit error rate.

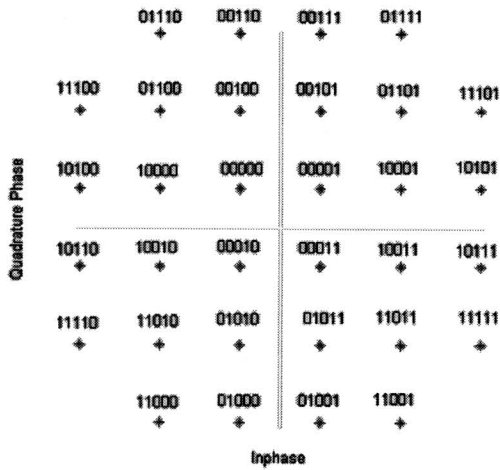


Figure 7 - Cross 32-QAM Symbol-to-Bit Mapping

5. RESULTS AND DISCUSSION

Bit error rate measurement and scatter plots were taken at each of the five different input backoffs of the Ka-band TWTA. Figure 8 shows the 1 Gbps 32-QAM scatter plot measured at the output of the modulator board with SRRC pulse-shaping bypassed. This was done to provide a clear picture of the transmit constellation; in all other results presented in this paper, the SRRC filter was enabled in the FPGA.

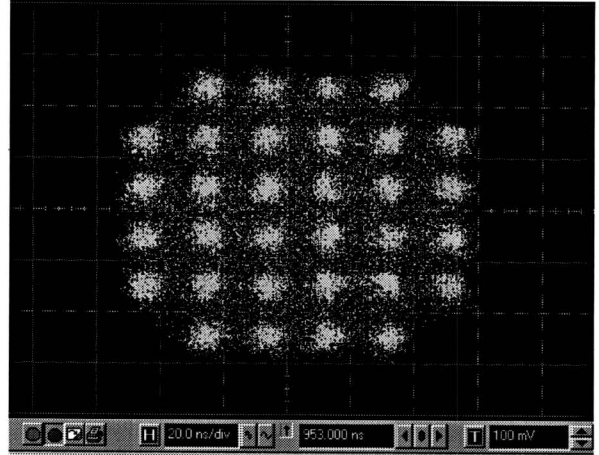


Figure 8 - 1 Gbps 32-QAM Transmit Constellation

Figure 9 shows the software receiver scatter plots of the output of the matched SRRC filter before and after RLS equalization with -8 dB IBO (linear operating point). Note that even at the linear operating point, there is sufficient hardware distortion that an equalizer is still needed to restore the constellation to its original shape.

Figure 10 shows the scatter plots of the matched filter outputs before and after the equalizer with $+5$ dB IBO (3 dB compression operating point). Notice in this case that even after equalization, significant distortion remains. This ends up creating an irreducible error floor as seen in Figure 11, but can be solved with modulator predistortion or using a linearizer.

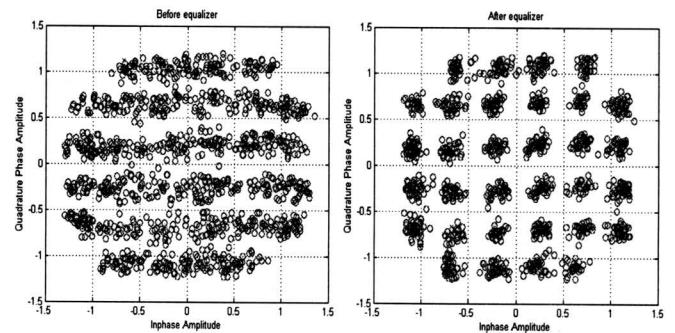


Figure 9 - Receiver Matched Filter Output Scatter Plot with -8 dB IBO: Pre-Equalization (left) and Post-Equalization (right)

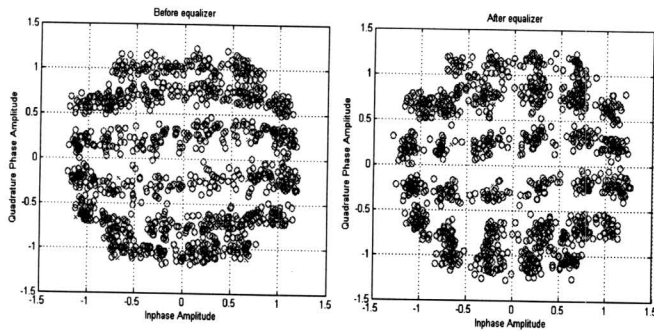


Figure 10 - Receiver Matched Filter Output Scatter Plot with +5 dB IBO: Pre-Equalization (left) and Post-Equalization (right)

Figure 11 shows the measured bit error rate for the different values of TWTA IBO. The theoretical BER for cross 32-QAM is shown in the figure for comparison. Preliminary simulation results indicate that even with the signal distortion, the bit error rate threshold prior to error correction is likely to be in the region between 5×10^{-2} BER and 5×10^{-3} BER depending on the strength of the punctured convolutional codes).

When the TWTA was operated at -8 dB IBO, the BER degradation from theory is roughly 3 dB at 5×10^{-2} BER and 5 dB at 5×10^{-3} BER. At -2 dB IBO and 0 dB IBO, the loss compared with theory at the higher BER threshold remains approximately the same compared with -8 dB IBO, while the loss at the lower BER threshold is about 1 dB greater. While these losses are large, they are not unusual for Gbps-type systems, and indicate the importance of error correcting coding and modulator predistortion when using high order modulations over a satellite channel. A summary of the test results can be found in Table 5.

For the saturated TWTA cases of +2 dB IBO and +5 dB, an error floor is noticeable where the distortion is large enough to cause errors even under virtually noiseless conditions. These results indicate that operation of SRRC 32-QAM up to the 1 dB compression point is possible; however above the 1 dB compression point, the distortion may be too severe for reasonable operation. Thus, operating at the 1 dB compression point (0 dB IBO) seems to be a good compromise between maximizing TWTA output power and avoiding excessive losses due to signal distortion.

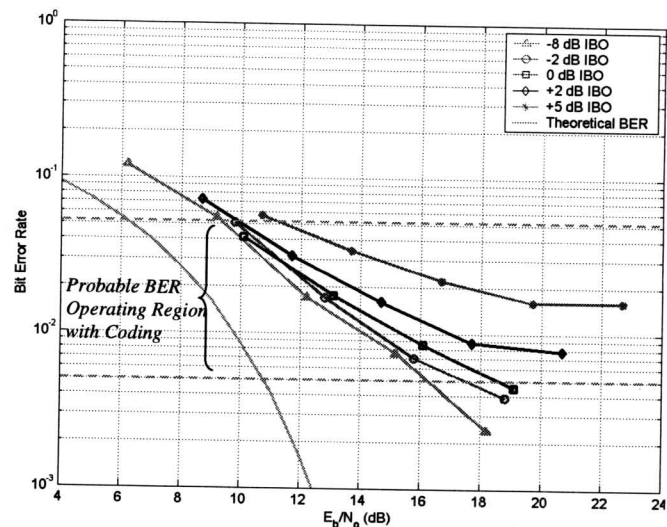


Figure 11 – Experimental SRRC 32-QAM BER Results for Different TWTA Input Backoffs

One Gbps 32-QAM Link Budget Examples

Link budgets are presented for two likely scenarios

The link scenario in Table 2 is for an Earth science LEO satellite at 300 km altitude transmitting a 1 Gbps 32-QAM telemetry downlink. The carrier frequency is assumed to be 26.7 GHz, and the power amplifier is assumed to be a 1W TWTA with AM/AM characteristics identical to the one used in the demonstration (see Figure 4). Based on results of the experiment, a TWTA input backoff of 0 dB was selected, and the resulting output power backoff and measured system loss values (from Figure 11) are entered into the link budget calculation. The receiving ground antenna is assumed to be a 5.4 meter Ka-band antenna at Wallops Flight Facility, already developed as part of the Ka-band Transition Project (KaTP) [4]. The receiver system noise temperature (SNT) is assumed to be 500 degree Kelvin. In order to satisfy the link, the spacecraft is assumed to carry a Medium Gain Antenna (MGA) with 25 dBi gain (conversely, the antenna gain can be reduced by increasing the TWTA power). The 1 Gbps 32-QAM signal is assumed to be trellis-coded with a required E_b/N_0 of 10 dB for a 10^{-6} BER, based on published simulation results [5]. Table 2 shows that under these hypothetical conditions, the 1 Gbps 32-QAM link from an Earth science LEO to the GN exceeds the required E_b/N_0 by 3.2 dB.

Table 2. Sample 1 Gbps 32-QAM Ka-band Link Budget Calculation for 300 km LEO to GN

Max TWTA Output Power (1W)	+30.0	dBm
TWTA output backoff ³	-5.0	dB
S/C Antenna Gain (est. MGA)	+25.0	dB _i
S/C Antenna eff (est. 70%)	-1.5	dB
S/C Pointing Loss (est.)	-1.0	dB
Space loss at 300 km @ 26.7 GHz	-170.5	dB
Atmospheric Attenuation (est.)	-1.0	dB
Ground Station Antenna Gain (5.4 meter dish)	63.6	dB _i
GS Antenna eff (est. 70%)	-1.5	dB
GS Pointing loss (est.)	-1.0	dB

Received Signal Power, P _r	-62.9	dBm
1/Bit Rate	-90.0	dB
1/N ₀ (est. SNT =500 deg K)	171.6	Hz/dBm
Received E _b /N ₀	18.7	dB

Ideal 32-QAM E _b /N ₀ for 10 ⁻⁶ BER, with trellis code (est)	10.0	dB
System loss including transmitter and channel distortions (Fig. 7)	5.5	dB
Required E _b /N ₀	15.5	dB

Margin	3.2	dB

Table 3. Sample 1 Gbps 32QAM Link Budget for 26 GHz Lunar Comm to 34m DSN Antenna

Max TWTA Output Power (100 W)	+50.0	dBm
TWTA output backoff ²	-5.0	dB
S/C Antenna Gain (est. 1m HGA)	+49.0	dB _i
S/C Antenna eff (est. 70%)	-1.5	dB
S/C Pointing Loss (est.)	-1.0	dB
Space loss from Moon @ 26.7 GHz	-232.7	dB
Atmospheric Attenuation (est.)	-1.0	dB
Ground Station Antenna Gain (34 meter dish)	79.6	dB _i
GS Antenna eff (est 70%)	-1.5	dB
GS Pointing loss (est.)	-1.5	dB

Received Signal Power, P _r	-65.6	dBm
1/Bit Rate	-90.0	dB
1/N ₀ (est. SNT =63 deg K + Lunar noise = 240 deg K)	173.8	Hz/dBm
Received E _b /N ₀	18.2	dB

Ideal 32-QAM E _b /N ₀ for 10 ⁻⁶ BER, with LDPC (est)	8.0	dB
System loss including transmitter and channel distortions (Fig. 7)	5.5	dB
Required E _b /N ₀	13.5	dB

Margin	4.7	dB

The second link scenario, presented in Table 3, is for a 1 Gbps 32-QAM communications link from a manned mission on the Moon to a 34m Beam Waveguide (BWG) antenna in the DSN. It should be noted that the DSN does not currently have 26 GHz receive capability. The transmit antenna on the Moon is assumed to be a 1-meter dish antenna. The transmit frequency is 26.7 GHz. A 100W TWTA is used in this scenario because of the longer range compared with the LEO link, but the same AM/AM characteristic and TWTA backoff is assumed as before. Based on the DSN 34m BWG system noise temperature at 32 GHz, the ground station SNT is estimated at 63 deg K. The Moon itself emits radiation (i.e., hot body noise) which will be received by the antenna since it is pointing at the Moon. If the antenna is pointed directly at the Moon, lunar hot body noise will increase the noise temperature by an estimated 240 K [6]. A LDPC code is used in the lunar communications scenario instead of a trellis code, and provides 2 dB more coding gain. Table 3 shows that under these hypothetical conditions, the 1 Gbps 32-QAM link from a lunar mission to the DSN would exceed the required E_b/N₀ by 4.7 dB.

³ Assuming 1dB IBO and the TWTA AM/AM characteristic in Figure 4.

6. CONCLUSION

This paper describes the end-to-end demonstration of a 1 Gbps communications link at 26 GHz using a high rate reconfigurable FPGA modulator. The experiment demonstrates the feasibility for NASA to transmit ultra-high data rates at Ka-band using very bandwidth efficient modulations (up to 5 bps/Hertz). Furthermore, it validates the flexible, relatively low-cost benefits of the high speed FPGA-based baseband modulator parallelized architecture jointly developed by JPL and GSFC. Potential target applications for the 1 Gbps 32-QAM link would be high rate telemetry from a LEO Earth science mission or from a manned lunar mission.

An RF experimental testbed was created which allowed for the characterization of spectral and BER performance of the 1 Gbps signal with realistic Ka-band (26 GHz) hardware distortions. In the future, the testbed will be used for additional Ka-band experiments with different modulation formats such as 8-PSK and 16-QAM, and various receiver architectures.

The benefits of using higher order modulations are illustrated in Table 4, which compares the bandwidths needed to achieve the target 1 Gbps data rate using the

same SRRC pulse-shaping. With SRRC 32-QAM, bandwidth required for 1 Gbps is 60% less than the 675 MHz bandwidth required by QPSK with identical SRRC pulse shaping.

Table 4. Bandwidth Required for 1 Gbps Data Rate

Modulation	Theoretical 2-sided BW for 1 Gbps with SRRC pulse shaping ($\alpha=0.35$)
BPSK	1.35 GHz
QPSK	675 MHz
8-PSK	450 MHz
16-QAM	337.5 MHz
32-QAM or 32 APSK	270 MHz

Spectral measurements of the 1 Gbps signal at the output of the Ka-band TWTA showed that the increase in the occupied bandwidth is minimal for power amplifier operating points up to the 1 dB compression point. Meanwhile, BER measurements showed losses ranging from -3 dB to -7.5 dB for operating points at or below the 1 dB compression point. Above the 1 dB compression point, an error floor was evident above 10^{-3} BER due to distortion from the TWTA non-linearity. While these losses are large, they were not unexpected and point to the use of error correcting codes and modulator predistortion as a necessity for very high data rate links at Ka-band.

Table 5 summarizes the BER degradation, output power backoff, and spectral regrowth (as measured by the 99% occupied bandwidth) as a function on TWTA input power backoff. By combining the TWTA output power reduction due to input backoff with the degradation at the specified BER threshold, this determines the total power loss at each input backoff value. Thus the optimal TWTA operating point can be determined by selecting the row with the lowest total power loss. For the 5×10^{-3} BER threshold, the 1 dB compression point (i.e., 0 dB IBO) is the optimum operating point. For 5×10^{-2} BER threshold, the 3 dB compression point maximizes the margin. However, due to the large amount of spectral regrowth as shown by the increase in occupied bandwidth in the last column, it would be recommended that the operating point remain at or below the 1 dB compression point.

Two areas for further work show great promise in improving the performance of the 1 Gbps system. The integration of advanced error correcting coding techniques to the experimental testbed should significantly improve performance. In particular, Low Density Parity Check (LDPC) codes and a trellis coding have been selected for further investigation with 32-QAM. Modulator predistortion can be used to mitigate effects of amplifier non-linearity and other transmitter hardware distortions. With the FPGA modulator architecture, this can be

implemented fairly easily in the testbed.

In conclusion, we would like to note that modeling and testing exact specifications of a proposed mission communications system is an important step in order to gain a mature understanding of a system. This in turn can be used to develop cost-effective end-to-end and component requirements. Such model-test-validate activities can produce very high return-on-investment.

REFERENCES

- [1] R. Porter, "NASA Infrastructure Capabilities to Support Near-Earth Missions", Wideband Downlink Briefing, Linthicum Heights, Maryland, July 2002.
- [2] W. Fong, A. Gray, and P. Yeh, "Bandwidth Efficient Baseband Multi-Modulator", Earth Science Technology Conference, College Park, Maryland, June 2003.
- [3] P. Vitthaladevuni and M. Alouini, "Exact BER Computation for the Cross 32-QAM Constellation", First International Symposium on Control, Communications, and Signal Processing, 2004.
- [4] Y. Wong and M. Burns, "NASA/GSFC Ground Segment Upgrades for Ka-band Support to Near-Earth Spacecraft", SpaceOps 2002, Houston, Texas, October 2002.
- [5] C. Dimakis, S. Kouris, and S. Avramis, "Performance Evaluation of Concatenated Coding Schemes on Multilevel QAM Signaling in Non-Gaussian Products Environment", IEE Proceedings, Vol. 140, No. 4, August 1993.
- [6] S. Slobin, "Atmospheric and Environmental Effects", DSMS Telecommunications Link Design Handbook, Document 810-005, Rev. E, February, 2003.

Table 5. 1 Gbps 32-QAM Summary of TWTA Operating Point Tradeoff

TWTA IBO ⁴	Occupied RF Bandwidth	TWTA Output Power Loss ⁵	Measured E_b/N_0 Loss at 5×10^{-2} BER ⁶	Total Power Loss at 5×10^{-2} BER ⁷	Measured E_b/N_0 Loss at 5×10^{-3} BER ⁶	Total Power Loss at 5×10^{-3} BER ⁷
-8 dB	247.5 MHz	-12 dB	-3 dB	-15 dB	-5 dB	-17 dB
-2 dB	250 MHz	-7 dB	-3.25 dB	-10.25 dB	-6.5 dB	-13.5 dB
0 dB	250 MHz	-5 dB	-3.25 dB	-8.25 dB	-7.5 dB	-12.5 dB
+2 dB	257.5 MHz	-4 dB	-3.5 dB	-7.5 dB	N/A	N/A
+5 dB	335 MHz	-2 dB	-5 dB	-7.0 dB	N/A	N/A

BIOGRAPHY

Dennis K. Lee (S'97 M'98) earned his B.S. from Case Western Reserve University in 1997 and his M.S. from Rensselaer Polytechnic Institute in 1998, both in Electrical Engineering. Since 1999, he has been a member of technical staff in the Digital Signal Processing Research group at the Jet Propulsion Laboratory. He has worked on several JPL missions including the Gravity Recovery and Climate Experiment (GRACE), the Dawn mission, and the Mars Reconnaissance Orbiter (MRO). He is also actively involved in the CCSDS RF and Modulation working group. Currently, his research interests include bandwidth efficient and multi-carrier modulations, and ultra-high bit rate communications.

Andrew Gray is a group supervisor of the Advanced Signal Processing Projects group in the Communications Architectures and Research Section, and co-coordinator for the forward-looking Eureka Process that resides in the Mission and System Architecture Section at the Jet Propulsion Laboratory (JPL). Andrew earned his MBA and PhD in electrical engineering from the University of Southern California in 2004 and 2000 respectively, his MS in electrical engineering from the Johns Hopkins University in 1997, and his BS in electronics with minor in mathematics in 1994.

Haiping Tsou Dr. Haiping Tsou received his B.S.E.E. degree from National Taiwan University, Taiwan in 1983, and his M.S.E.E. and Ph.D. degrees from University of Southern California in 1992. He joined Jet Propulsion Laboratory in 1992 and, since then, has been involved in researches on digital receiver design, modulation, synchronization, detection, and signal processing for



deep space communications. His current interests include bandwidth efficient modulations in multipath fading environments and pointing-and-tracking techniques in free-space optical communications.

Edward Kang (S'84) earned his B.S. from University of California at Los Angeles 1984 in Electrical Engineering. Since 2000 he has been a member of technical staff in the Advanced Signal Processing Projects group at the Jet Propulsion Laboratory. Mr. Kang is currently a design engineer for JPL's Mars Laser Communications Demonstration (MLCD) ground optical receiver.

Norman Lay received the B.S.E.E. degree from Columbia University, New York, NY, in 1983 and the M.S.E.E. degree from Stanford University, Stanford, CA, in 1984. From 1984 to 1986, he was employed at the General Electric Corporation Research and Development Center, Schenectady, NY. During this period, he worked on a variety of signal processing applications including speech compression, pilot-aided digital modulations, and digital control systems. Since 1986, he has been at the Jet Propulsion Laboratory, Pasadena, CA, where he has worked primarily in the area of digital modem development for mobile satellite systems. He is currently a group supervisor in the Communications and Systems Research Section.

⁴ TWTA IBO is measured relative to TWTA 1 dB compression point

⁵ TWTA Output Power Loss is measured relative to maximum TWTA output power

⁶ E_b/N_0 Loss is measured with respect to ideal 32-QAM at specified bit error rate

⁷ Total Power Loss is the sum of the E_b/N_0 Loss and the TWTA Output Power Loss